

ECG:

Circuit Design:

The circuit design for obtaining the ECG signal were limited by constraints of ultra low power and ultra portability, wearable design philosophy and small physical dimensions. The system was divided into 4 major parts : Power, Analog Front End, Communications and User Interface. The designed system could be used on a as-is basis or extended to measure other small bio potential signals.

Analog Front End:

The Analog Front End is the most essential part of the system. It is responsible for signal integrity and precise measurement of the ECG signal. The amplitude of the ECG signal lies in the range : 0.1mV- 1mV, and the bandwidth lies in the range from 0.2 Hz to 200 Hz. The AFE must be able to reject Common-mode noise. The most critical component of the AFE is the amplifier which is used to amplify the ECG signal without adding much noise. Other significant parts of the AFE include suitable low pass filters to remove high frequency noise and notch filter at 50-60Hz to remove power hum.

Communication:

The raw ECG signal must be transmitted to a User interface for further processing to aid in patient monitoring and diagnosis. The communication block receives the raw ECG signal, carries out the Analog to Digital conversion and transmits the data to the User Interface. The amplitude of the ECG signal is rather small even after amplification and is converted from analog to digital domain using a Successive Approximation (SAR) ADC of 12 bit precision. Bluetooth was chosen as a means of transmitting the data from the communication block to the User Interface to make the system wireless and provide a hassle free and user-friendly experience. This will also allow the system to connect to a range of user platforms without any modification to the hardware. The .An atmel Atmega 328P- 16 Mhz surface mounted micro controller was programmed to read the analog signal, carry out the Analog to digital conversion and transmit the data over serial bluetooth line via a HC-05 Bluetooth module.

Power:

The selection of the power source for the designed system was based on low power and portability restraints of the system. The power block for the ultra low power ECG monitoring system should also fulfill the requirements of basic safety, portability, maximum lifetime, minimum storage requirement and the size constraints of the system. The battery life should be sufficiently long so that the user does not have to worry about charging the device often. A simple Cr232 button cell was first investigated as a possible power source but it was quickly discarded in favor of a commercially available rechargeable GT-08 Lithium Polymer Smartwatch battery-380mAh due to the current draw requirements and insufficient life time. The smartwatch battery should last a few days in continuous operation. The power profile of the designed system is investigated further in the text.

User Interface:

The user interface should allow easy, real time and continuous monitoring of the ECG signal. The primary user Interface was developed for the desktop using Java Processing to display the data

obtained from the hardware. The ECG and PPG signal were plotted in real time. The heart rate was calculated from both the ECG and PPG signal. The Inter beat interval was calculated from the PPG signal and the QRS wave component in the ECG signal was also identified. After testing the hardware on the desktop platform , a cross platform mobile application was designed to plot both the ECG and the PPG signal in real-time. The data was also saved in separate csv files on the mobile phone for further processing . The data can also be transmitted to a server over WLAN or 3G internet for further processing, however this part is not covered in the scope of this project.

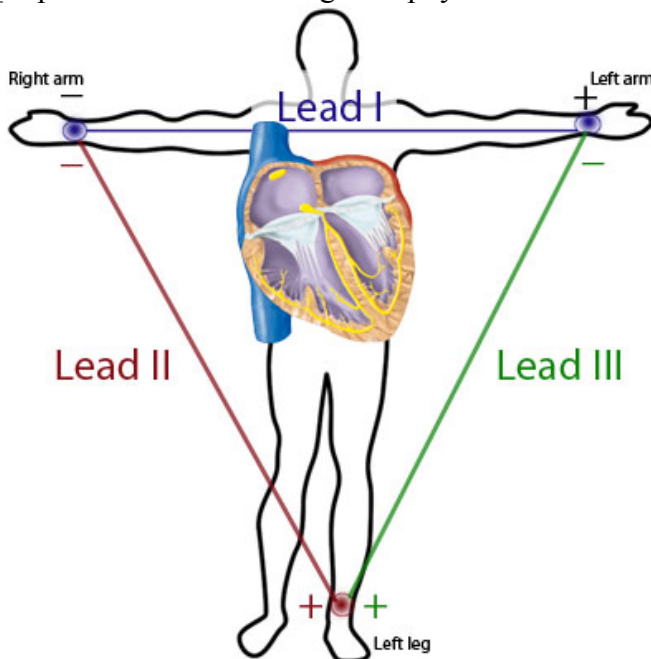
Analog Front End:

ECG is a very weak and noisy signal. The analog to digital converters cannot process an un-amplified ECG signal due to its small amplitude. For proper signal acquisition an appropriate analog front end must be designed to amplify the small ECG signal and further condition the signal before it is fed into the system's ADC. The AFE must also compensate for noise interference and motion artifacts present in the ECG signal. This process is known as signal pre-conditioning. The signal preconditioning stages comprises of extraction, amplification and filtering stages.

Extraction of the ECG signal:

Most ECG machines have 2 or more electrodes , which monitor the voltage across one or more leads. Clinical standard uses a 12-lead ECG . It provides a detailed view of the heart's electrical activity from different points on the body. Each lead corresponds to a vector of ECG electrical potential. The electrodes are typically placed in a setup known as the Einthoven's triangle.

Willem Einthoven (1860-1927) explained the principles of the ECG in scientific terms. The standard connections for all three limb leads are shown to the left below. In Einthoven's triangle, the heart may be considered to lie at the centre of an equilateral triangle and the corners of the triangles are the effective sensing points - the right arm(RA), left arm (LA)and left leg (LL)electrodes.
[<http://www.medicine.mcgill.ca/physio/vlab/cardio/setup.htm>]

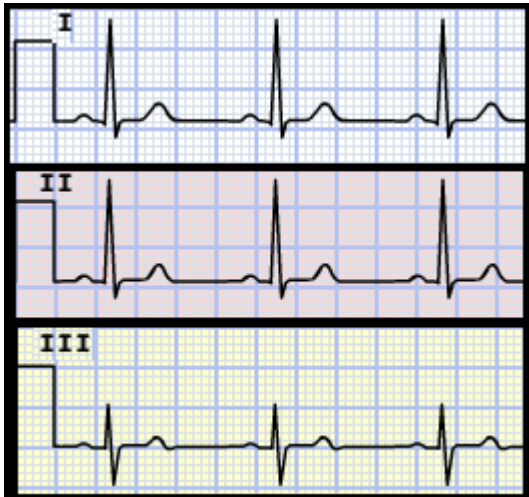


$$\text{Lead I} = (V_{LA} - V_{RL}) - (V_{RA} - V_{RL}) = V_{LA} - V_{RA}$$

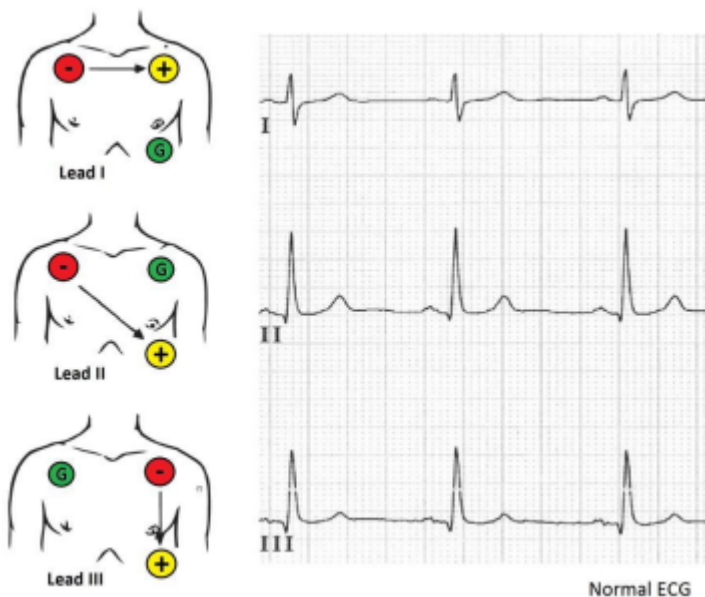
$$\text{Lead II} = (V_{LL} - V_{RL}) - (V_{RA} - V_{RL}) = V_{LL} - V_{RA}$$

$$\text{Lead III} = (V_{LL} - V_{RL}) - (V_{LA} - V_{RL}) = V_{LL} - V_{LA}$$

The signal received from each lead on a FDA approved standard ECG machine are shown in figure below:



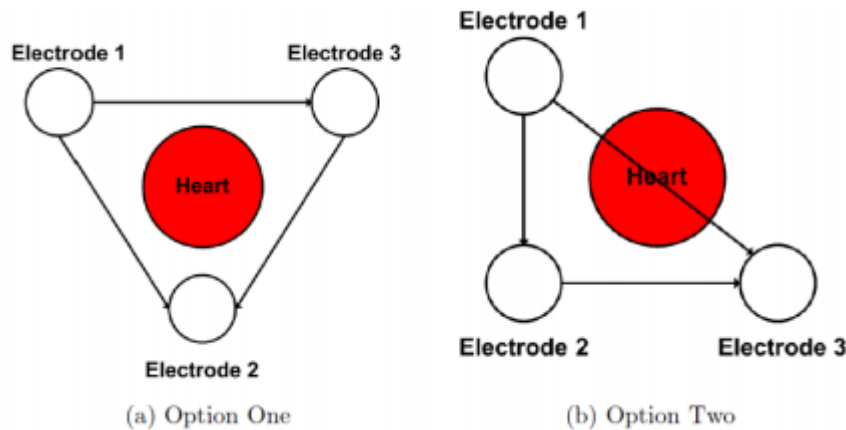
Since each lead corresponds to a vector of ECG electrical potential, different ECG signals can be obtained from different lead locations. The corresponding ECG signals from different lead locations is shown in the figure below:



The most important characteristic of the ECG signal for our purpose is the positive R-wave. It can be seen in the figure above that lead II configuration provides the largest positive R-wave and is therefore selected as the desirable lead configuration for this project.

Three electrode configuration:

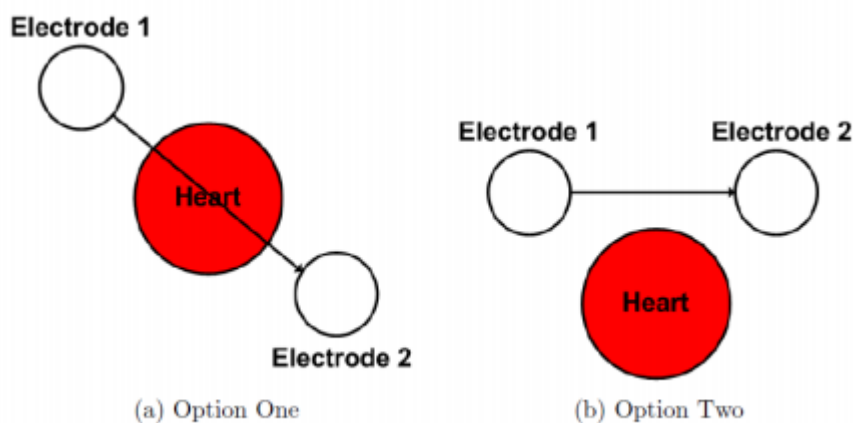
It is possible to have upto 3 unique vector for three electrodes. Two electrodes are used to form a vector and the third electrode provides a reference. This configuration allows more lead selection options and eventually less noise disturbance in the signal. The possible locations for three electrode configuration are shown in the figure below:



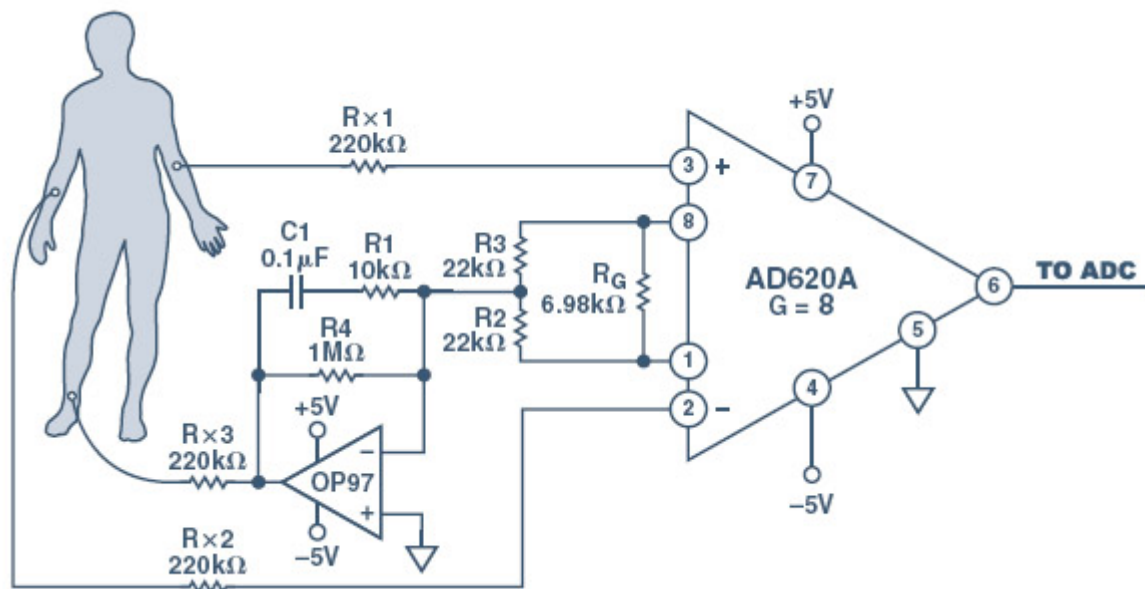
Configuration I is preferred in clinical studies as it offers a good of Leads I, II and III. However, configuration II is preferred for patient comfort but it only provides a good view of lead II. A right leg drive electrode (electrode 3) is used to bias the subject to set a DC operating point determined by the operating voltage of the monitoring system. Data from lead I and lead II cannot be reliably obtained from this configuration. Important information regarding the electrical operation of the heart muscle is lost with the loss of 2-leads . But the R-wave can still be observed with this limited view.

Two Electrode Configuration:

With the two electrode configuration it is only possible to have a good view of only 1 lead. The two electrode configuration is shown in the figure below: Configuration I allows a good view of the Lead II and configuration II allows a good view of the lead I. The two electrode configuration provides a smaller amplitude of signal when compared to the lead II in 3 electrode configuration . This might lead to difficulty in identifying useful features of the ECG signal such as P and U waves but the R-wave is easily identifiable with 2 electrodes in both configurations.



Since our ECG monitor is an ultra portable smartwatch type design we use configuration II with 2 electrode to obtain a good view of lead I in order to identify the R-peak. The electrodes were placed on the right and left wrist instead of the chest. This leads to interference from various muscle groups and a noisier signal, but the R-wave can still easily be identified with visual inspection or simple signal processing with electrode placement on both wrist. The equivalence of electrode placement on wrist instead of the chest was proven with the simple ECG circuit provided in the data sheet of AD620 amplifier shown below:



Credit: data sheet ad 620, Analog Devices

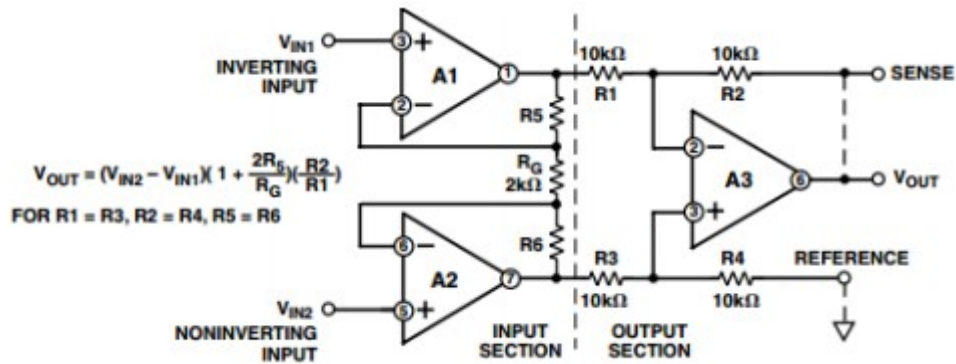
The reference circuit (shown in figure above) was constructed on a breadboard and the R-wave was identified first with the electrodes placed on the chest and then on the wrist. The sample circuit served as a valuable evaluation aid, but was quickly discarded for further use due to intensive power requirements. (It requires both -5 and +5 V to operate). The following ECG waveforms were obtained from the circuit shown above.

Requirements:

A detailed study of the requirements for a portable, low power ECG analog front end was carried out. It was found that the ECG monitoring system must be able to extract very low voltage signals in the range 0.1mV-1mV with a frequency range from 0.2-200 Hz. The system should allow both 2-electrode and 3-electrode configurations. It was noted that skin electrode contact is a source of interference which produces an offset of 200-300mV. The system should be able to cope with this interference and other sources of noise. The AFE should be able to run on 2-4 Volts. The area of the designed PCB and the power consumed should be minimized.

The AFE should be able to take 2 types of signals at the input: Common-mode signal (same potential) and differential-mode signal (differing potential). The common-mode signal is unwanted for ECG monitoring systems. The potential between the electrodes and ground can create a Common-Mode component of up to 1.5V [3] and the designed AFE should be able to cancel out the common-mode signal and amplify the differential-mode signal at the input. The ratio of change in output voltage to change in Common-Mode input voltage is known as the Common-Mode gain. The ratio of the differential gain to the Common-Mode gain is the Common-Mode Rejection Ratio (CMRR). The CMRR of the designed system should be 80dB to 120dB over the input frequencies that need to be rejected [3].

An instrumentation amplifier should be used to achieve sufficient gain and Common-Mode rejection. An instrumentation amplifier has a differential input and a single ended output with respect to a reference voltage. The in-amp gain is determined by external resistors that are connected between inverting input and the output [3]. The internal structure of a classic instrumentation amplifier with 3 operational amplifiers (op-amps) is shown in the figure below.



Design:

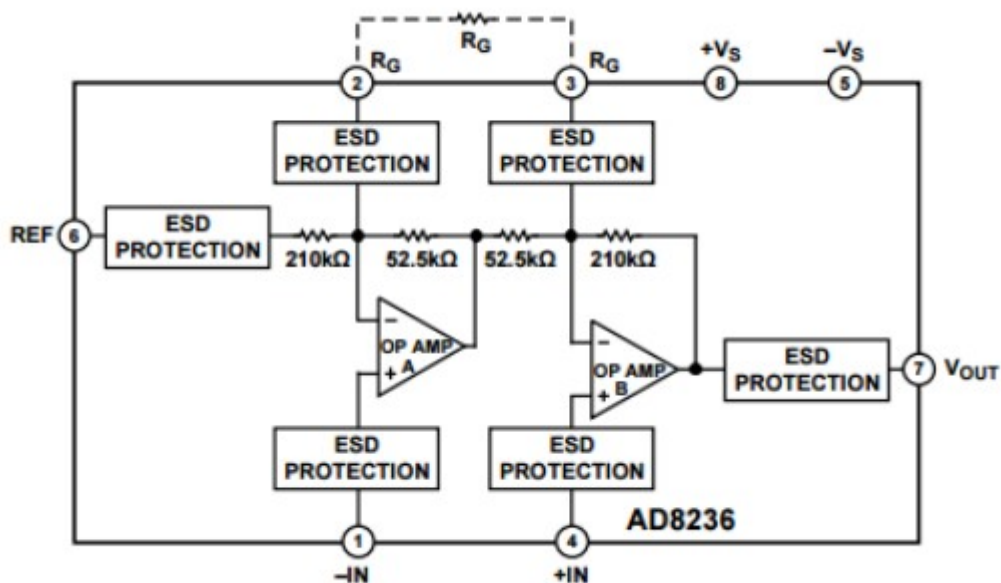
The data sheet for several application specific ICs and low power general instrumentation amplifiers were studied and their properties were evaluated for application in our design. A comprehensive comparison is presented in the following sections. The AD 8232 instrumentation amplifier was selected as the final choice for the AFE according to the discussion presented in the next section.

Instrumentation amplifiers:

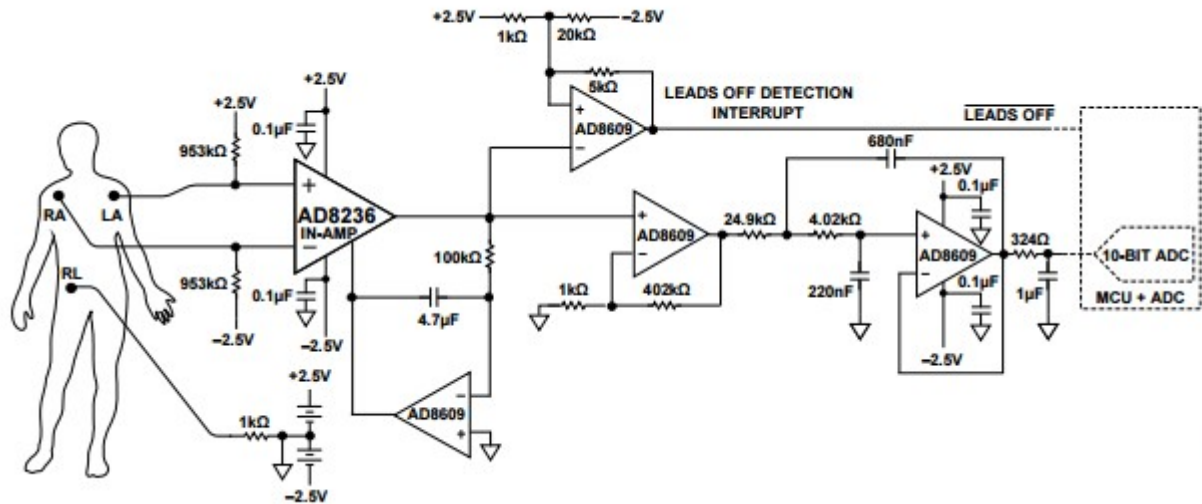
AD8236:

AD 8236 has the lowest power consumption among the instrumentation amplifiers available commercially. A simplified version of the AD8236 is shown in the figure below. It operates on a single power supply of 1.8 V- 3V. High input impedance, a minimum gain of 5, low input bias of 1pA and a relatively high CMRR of 110dB make it suitable for our design. The rail-to-rail input and output provides a wide dynamic range, which means that the maximum input or output swing is equal to the power supply voltage [3]. The output can be easily shifted according to individual application by applying a reference voltage to the REF pin. The shifted output can be easily integrated with the ADC. The default gain value of 5 can be reconfigured by placing a resistor across the RG pin. The additional gain can be set with respect to the resistor value. The resistor value for the desired gain can be calculated according to Equation below:

$$R = 420k/G - 5$$



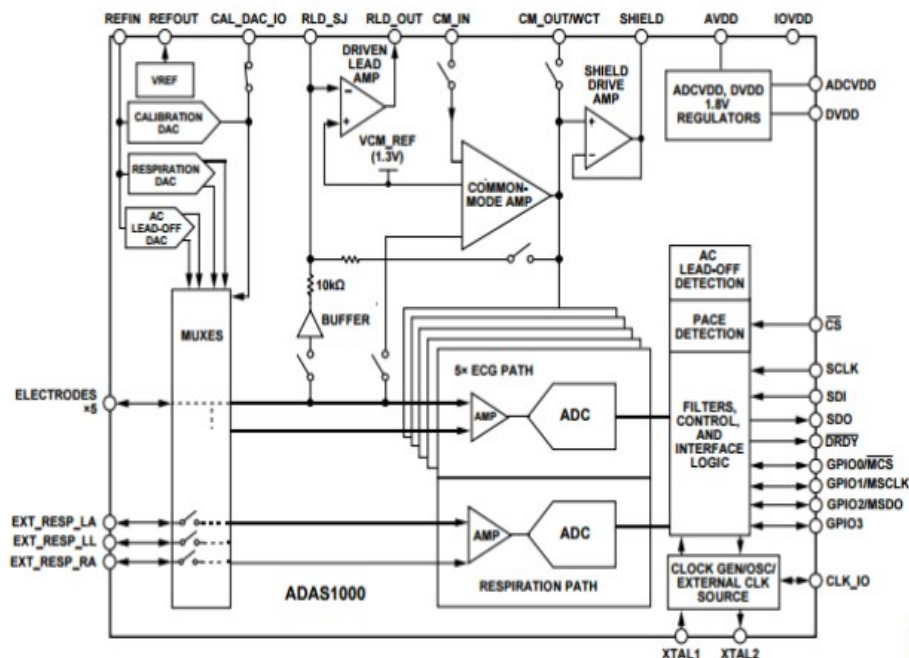
The AD8236 has DC overload protection, which allows a diode drop (approximately 0.7V) above the positive supply and a diode drop below the negative supply. It can handle a continuous current of 6mA. The relatively high CMRR (110dB) and the capability to remove any differential DC offsets (electrode half-cell potential) make AD8236 a good candidate for ECG monitoring system. A sample low power heart rate monitor is provided in the data sheet (shown below) which demonstrate the common application of this IC in ECG monitoring systems.



credit: data sheet ad 8236, analog devices

ADAS1000 :

The functional block diagram of the ADAS1000 is shown in Figure below.



credit: ADAS 1000 data sheet, analog devices

The ADAS1000 is a high-performance, low power analog front end (AFE) IC. It is widely used in monitoring ECG signal. It was designed according to the various clinical and electrical standards for electrocardiograph apparatuses. It can also measure thoracic impedance and pacing artifacts[5].

This makes it suitable for monitoring patients with surgically implanted pace makers and its electrical effects.[24].

The ADAS1000 has five acquisition channels and a Right Leg Drive (RLD). The right leg drive serves as a reference voltage. The channels are equipped with a differential pre-amplifier with configurable gain, a fixed gain 2-pole anti-aliasing filter, a 14 bit 2MHz ADC, and buffers. An anti-aliasing filter can detect pace artifacts. The Leads can be configured as either digital and analog.[5].

Power Consumption:

The ADAS1000 requires an operating voltage of 3.3V to 5V . The power consumption is shown for various electrode configurations are shown in the table below:

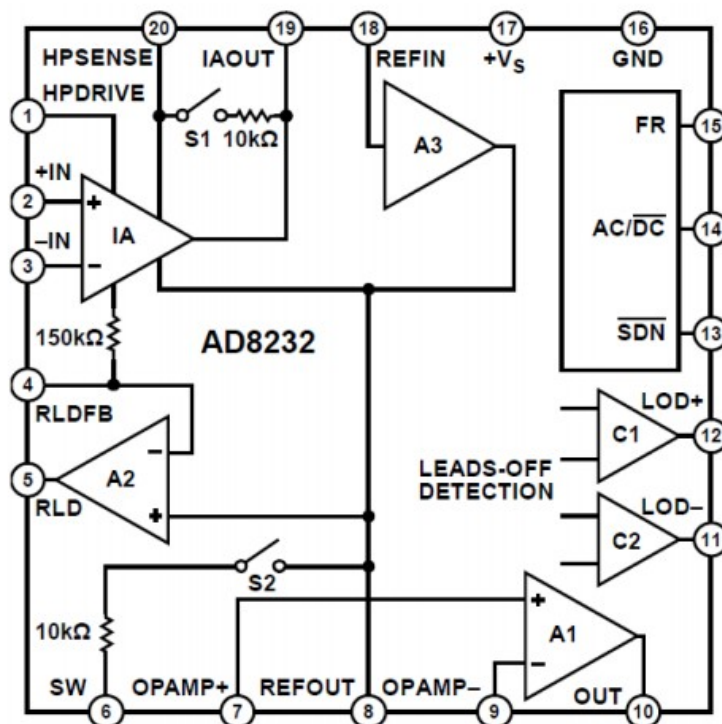
Electrode Configuraton	Power consumption
1-lead	11mW
3-lead	15mW
5-lead	21mW

The noise power can be reduced by increasing the power consumption. The power consumption can be reduced by enabling the power-down mode. In the power-down mode, the signal acquisition channels are switched off and the data rate is reduced.[5]. The ADAS1000 also offers the capability of AC and DC lead off detection.

A 8.192MHz crystal can be connected externally and the internal regulators can be used to drive the IC with a raw input. A power on self-test performs various critical operations such as : reading registers, Cyclic Redundancy Check (CRC) and calibration of the Digital to Analog Converter (DAC). The aquired data can be sent to a DSP or microcontroller through Serial interface SPI or QSPI at configurable data rates.

AD8232 :

The functional block diagram of the AD8232 is shown in Figure below:



credit:AD8232, data sheet Analog Devices

The AD8232 is another ultra low power instrumentation amplifier capable of acquiring and amplifying small bio signals. It can also remove motion artifacts and interference from electrode half cell potential. A leads off detection circuitry and fast restore capability is implemented in the AD8232 to reduce the recovery time if one of the leads is disconnected. The AD8232 comprises of four amplifiers: an instrumentation amplifier, an operational amplifier (A1), a Right Leg Drive (RLD) A2, and a buffer amplifier A3.

The AD8232 can be operated with both 2-electrode and 3-electrode configurations. The Right Leg Drive (RLD) serves as the reference lead in a 3-electrode configuration. The Right Leg Drive amplifier rejects the Common-Mode voltage at the input of the instrumentation amplifier. The AD8232 has a CMRR of 86dB. All terminals of the AD8232 are shielded against electrostatic discharge (ESD). External resistors can be utilized to avoid overload conditions at the input[6].

The instrumentation amplifier in the AD8232 has a fixed gain of 100. An operational amplifier is available for selectively low pass filtering the noise components in the signal. A low pass filter with a cutoff frequency of 1.1 Mhz is implemented at each input pin of the AD8232 to avoid RF interference[6]. This prevents a DC offset in the acquired signal.

A reference buffer is used to create a virtual ground (reference voltage) between the actual ground and the power supply. A voltage divider and an external power supply can be used to drive the reference voltage from REFIN pin. The virtual ground is available at REFOUT. The AD8232 provides AC and DC leads off detection. The connection at each input is checked using DC lead off detection in the three electrode configuration. If the IN+ electrode is disconnected the LOD+ pin is set and if the IN- is disconnected the LOD- pin is set.

For the 2-electrode configuration AC lead off detection is used. A high impedance AC signal is injected into the input terminals every few seconds. If the lead is connected the AC signal will be heavily attenuated, if it is not attenuated the lead has been disconnected.[6].

The AD8232 requires an operating voltage of 2-3.5V. It can be operated with CR2032 cell batteries or rechargeable lithium ion batteries. A power save mode with a current draw of less than 200nA can be enabled to minimize power consumption.[6].

Final Design :

The complexity, adaptability and portability of the three AFE blocks were compared. The features available in each AFE were evaluated according to design requirements. The ADAS1000 offers a lot of features but it requires more power. Additional features are packaged with greater complexity and a higher price. The AD8236 is a general purpose instrumentation amplifier with a very attractive power consumption profile. But it would require at least four other operational amplifiers to design the desired AFE. The additional amplifiers will increase the PCB footprint. An AFE designed with the AD8236 might be the most power efficient but it cannot be the smallest design in terms of physical dimensions. The AD8232 emerges as a clear winner, as it consumes less power than the ADAS1000. The AD8232 offers fewer features in comparison to the ADAS1000. However, this leads to reduced complexity. On the other hand, it offers more features than the AD8236. The AD8232 was therefore selected for the purpose of this project. The table below shows the most important features for comparison.

IC	Operating Voltage (V)	Operating current(micro ampere)	No. of electrodes	CMRR(dB) for gain values of 100
AD8232	2-3.5	170	3	86

AD8236	1.8-5.5	33	-	110
ADAS1000	3.15-5.5	785	5	110

Method:

A total of 30 patients participated in the study over the course of weeks. The patients were asked to fill out a medical history form [Survey 1]. 3 Blood pressure readings were recorded with the cuff based apparatus. The ECG and PPG signal were recorded with the smartwatch design. The patient was at rest and mentally relaxed. The subject then completed an exercise test with simultaneous heart rate , ECG and PPG data collection.

The exercise test comprised of riding a stationary bike with incremental load until exhaustion. 3 data points were obtained during the 10 min reference period. 5 data points were obtained during the exercise. 2 data points were obtained during the recovery period. The blood pressure readings were obtained from the right arm , using an automated oscillometric system.

Data Analysis:

The time synchronised ECG and PPG signal values were saved as a csv file on the mobile phone and uploaded to a PC for statistical analysis. The PTT was calculated for the R-wave in the ECG signal and the steepest slope of the PPG signal in Matlab. The beat to beat PTT values were filtered with a moving average filter, window length =30 sec.

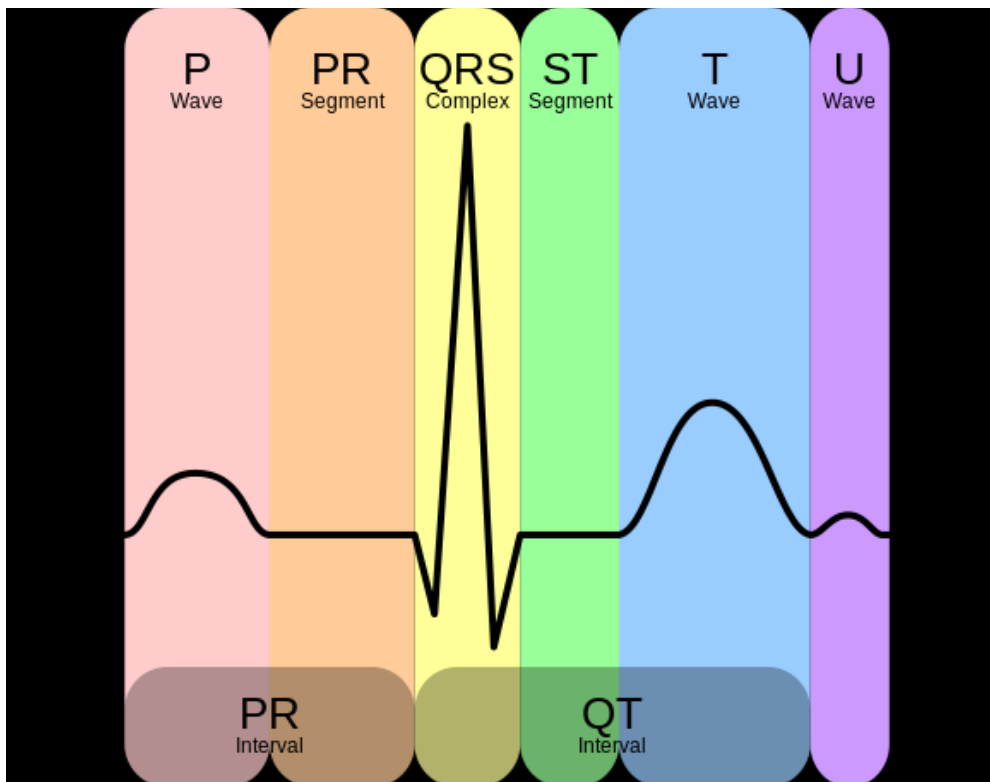
10 data pairs were selected for each subject.

Data pair	Description
T1,T2	Recorded at rest
T3	Recorded just before mounting the exercise bike
T4,T5	recorded during exercise
T6	Recorded at Peak exercise
T7,T8	Recorded after peak exercise
T9,T10	Recorded during recovery

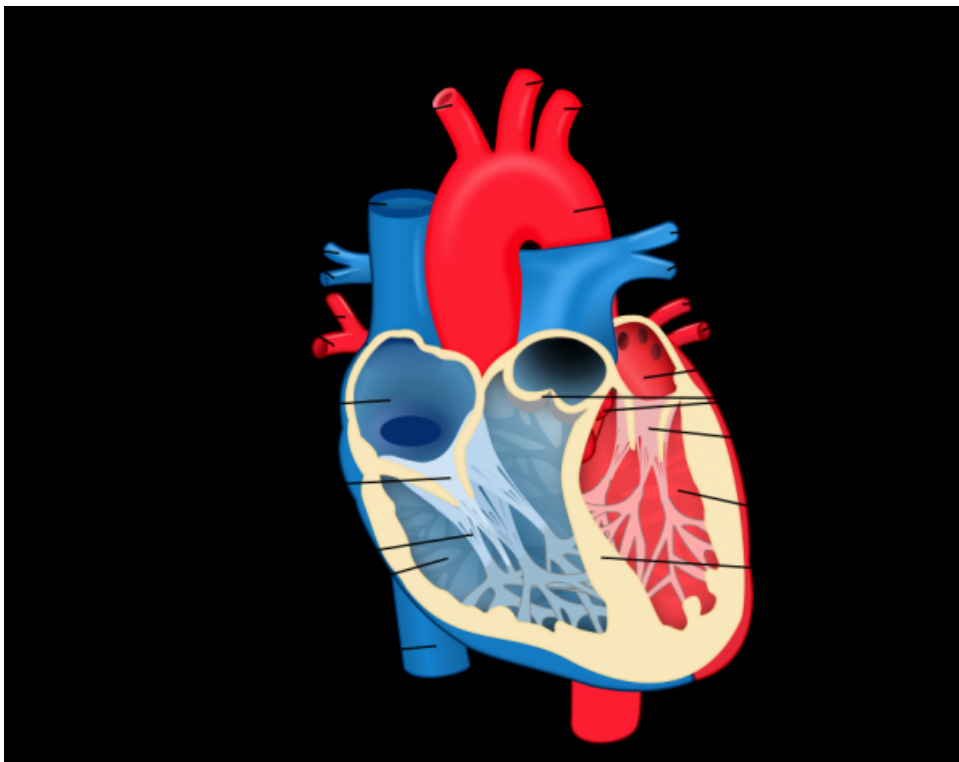
The blood pressure was measured at these points using the cuff based method. The time synchronised PTT value was assigned to each sample.

ECG signal:

The ECG signal comprises of the PR interval and the QT interval.



Credit : wikipedia.org



Credit : wikipedia.org

PR Interval:

Electrical impulses travel from the right atrium to the left atrium. The wave generated by this electrical impulse is known as the PR interval. The right and left atrium are “depolarized” during this interval . The right atrium is “depolarized” first and deoxygenated blood is drained into the right ventricle from superior and inferior vena cava. As the impulse travels from right atrium to left atrium, the left atrium contracts to receive oxygenated blood from the lungs into the left ventricle through both the pulmonary veins.

QT Interval:

Both ventricles begin to pump during the QRS . De-oxygenated blood is pumped by the right ventricle into lungs through both the pulmonary arteries. Oxygenated blood is pumped by the left ventricle into the rest of the body through the aorta. The ST interval has minimal electrical activity as the ventricles are “ re-polarized” by the T-wave. The T-wave causes the both the ventricles to relax. Blood enters the ventricles through the atria during the relaxation phase.

R-wave detection:

The ECG signal is non stationary as the frequency content varies over time. A QRS interval detector was implemented in Matlab as a general feature detector. Wavelet decomposition was used to decompose the ECG signal into time-varying frequency components. The signal components were separated into various frequency bands to generate a reduced representation of the signal. The “sym4” wavelet was selected to detect the QRS complex because it resembles the ECG signal [see Fig. Below].

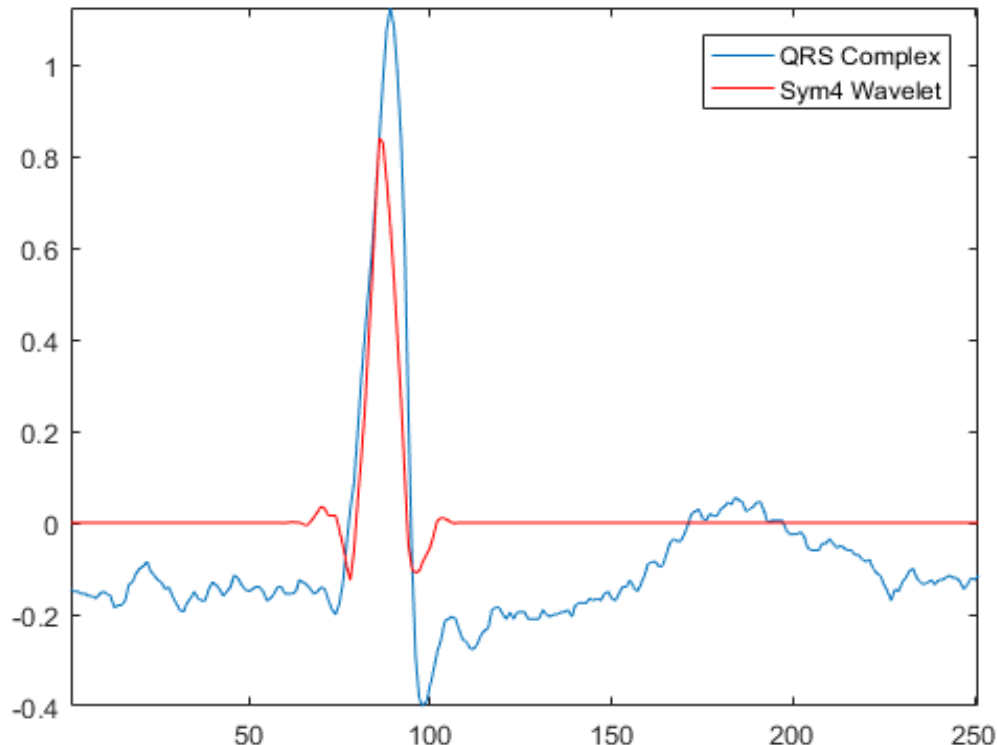


[Fig. QRS complex vs sym4 wavelet]

The following Matlab code was used to extract the R-wave.

```

load ecg;
figure
plot(time,ecgsig)
//hold on
//plot(time(ann),ecgsig(ann),'ro')
xlabel('Sec'); ylabel('Amplitude')
title('ECG signal Preprocessed')
qrsfd = ecgsig(560:810);
[mpdict,~,~,longs] = wmpdictionary(numel(qrsfd),'lstcpt',{{'sym4',3}});
figure
plot(qrsfd)
hold on
plot(2*circshift(mpdict(:,11),[-2 0]),'r')
axis tight
legend('QRS Complex','Sym4 Wavelet')
title('Comparison of Sym4 Wavelet and QRS Complex')
wt = modwt(ecgsig,5);
wtrec = zeros(size(wt));
wtrec(4:5,:) = wt(4:5,:);
y = imodwt(wtrec,'sym4');
y = abs(y).^2;
[qrspeaks,locs] = findpeaks(y,time,'MinPeakHeight',0.35,...
    'MinPeakDistance',0.150);
figure;
plot(time,y)
hold on
plot(locs,qrspeaks,'ro')
xlabel('Seconds')
title('R Peaks - |Wavelet Transform ')

```

A commercially available FDA approved Upper arm Electronic Blood pressure Monitor served as the control experiment. The equivalence of this apparatus to the gold standard method has been the subject of another study. [1-4]. The low power smartwatch type blood pressure monitor was used to record the PPG and ECG signals. The data was transmitted over Bluetooth to a Samsung Galaxy Note 4. The data was saved on mobile phone and uploaded to PC via USB for detailed statistical analysis. Time synchronised values of PTT were used to calculate the blood pressure. Charts.js and AngularJs were used to generate real time, interactive graphs. The data was analyzed using python, Matlab and LibreCalc. The relationship between blood pressure obtained from the gold standard method and PTT was analyzed by linear and nonlinear regression models.

Patient characteristics:

A total of 30 patients participated in the study [Table 1] .

[Table 1- Patient characteristics]

Characteristic	N=30
Age	44.1 +/- 20.2 years
Male,n %	19 (63.3%)

Body height, cm	170+/- 15.9
Body mass index kg/m2	24.6 +/- 7.2
History of smoking, n (%)	17 (56.6%)
History of hypertension, n (%)	8 (26.6%)
Diabetes mellitus, n (%)	3 (10%)

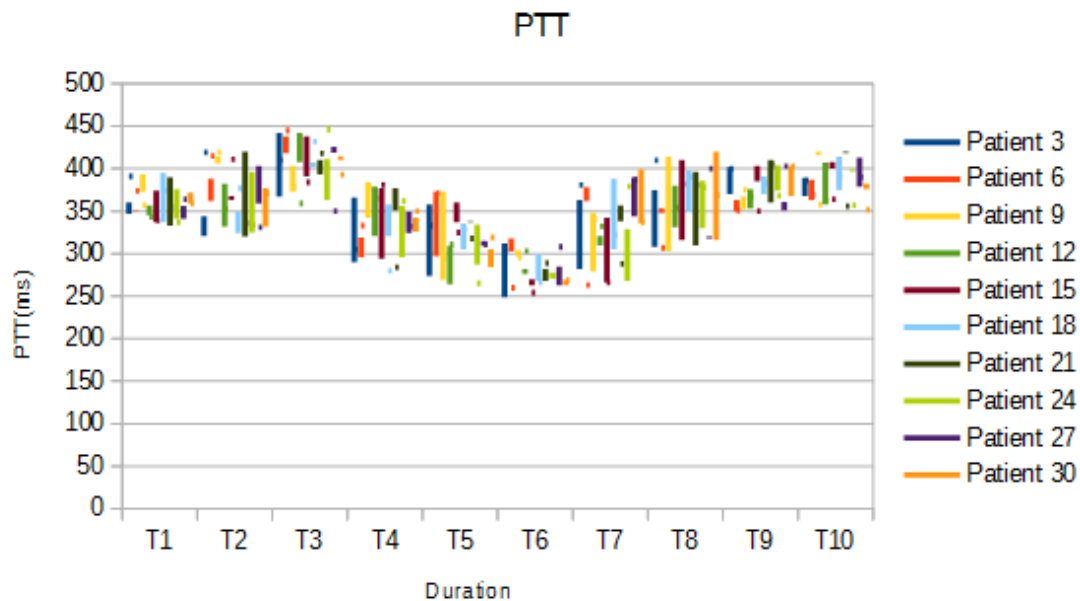
The majority of patients had no history of pulmonary diseases. One patient had a history of abnormal heart rhythm (patient 11). The data for these patients was not singled out in any manner and remains a part of the statistical analysis.

[Table 2]

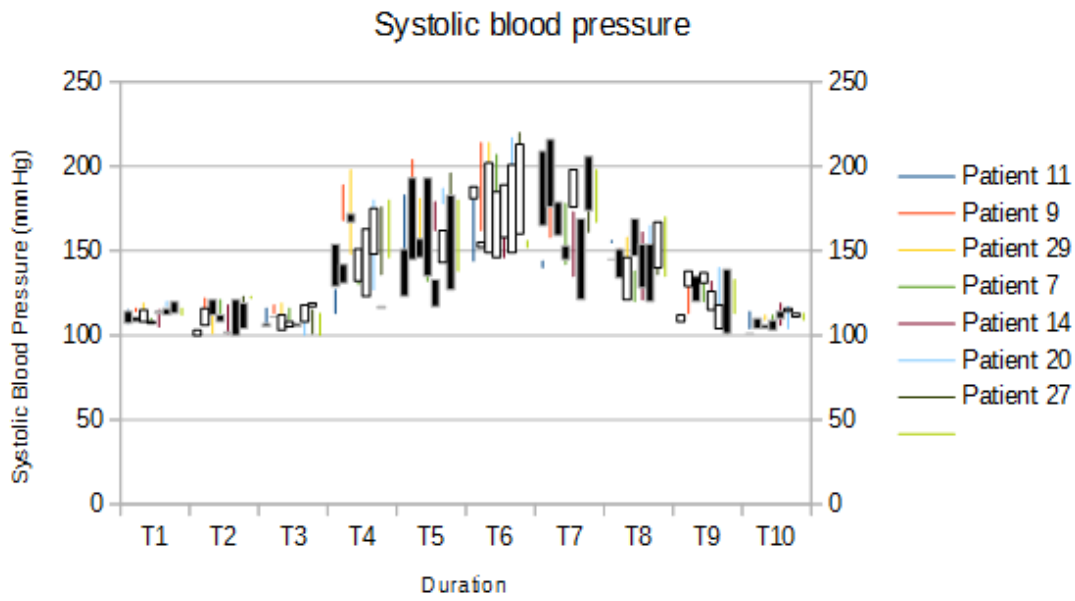
Anaerobic threshold workload,	91 +/- 48
Peak-VO2, ml/min/kg	20.3 +/- 9.4
VE/VCO2	35.8 +/- 6.8
Limitations to maximum exercise, n (%)	20
Evaluable BP/PTT pairs, n	20 +/- 0.3

Results:

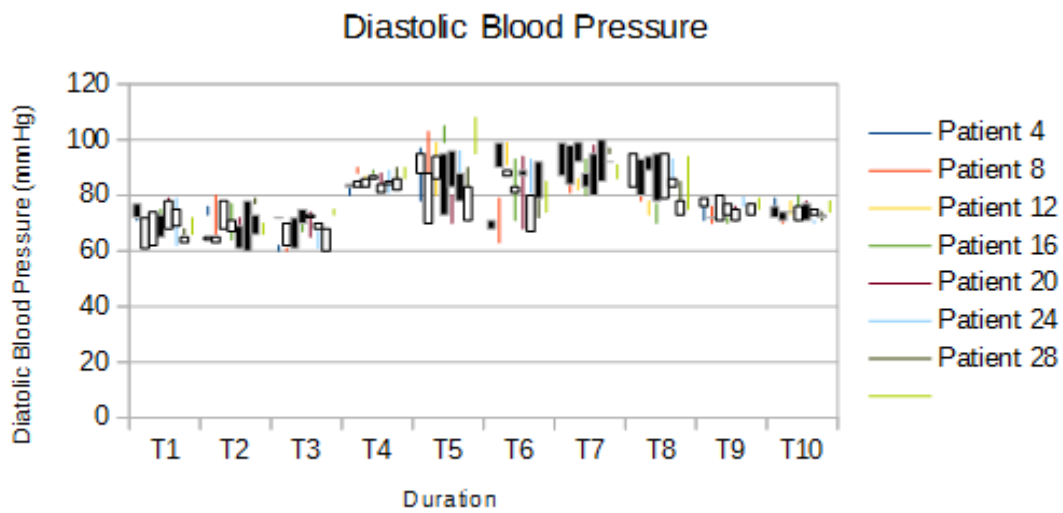
Results from the exercise tests and PTT measurements are shown in Fig 1-3.



(1a)

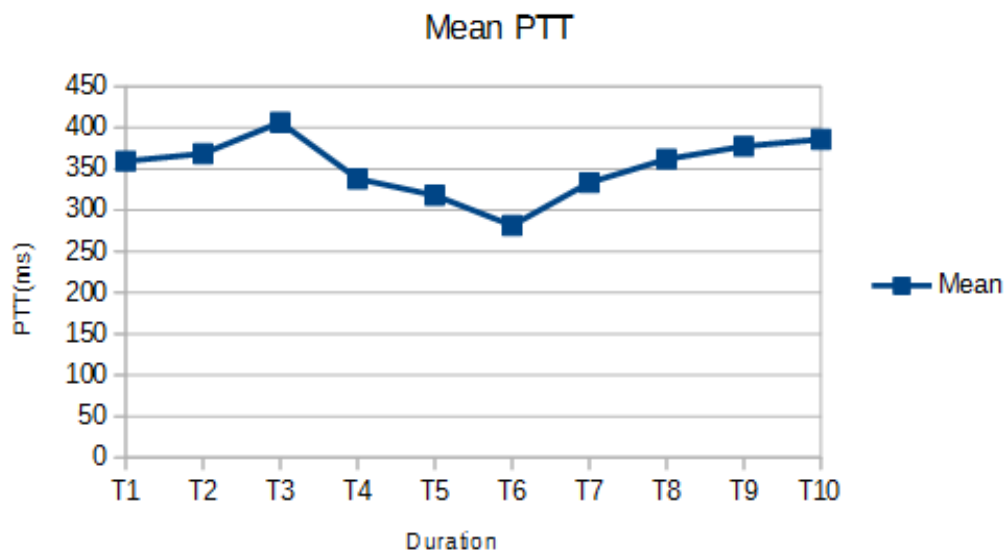


(1b)

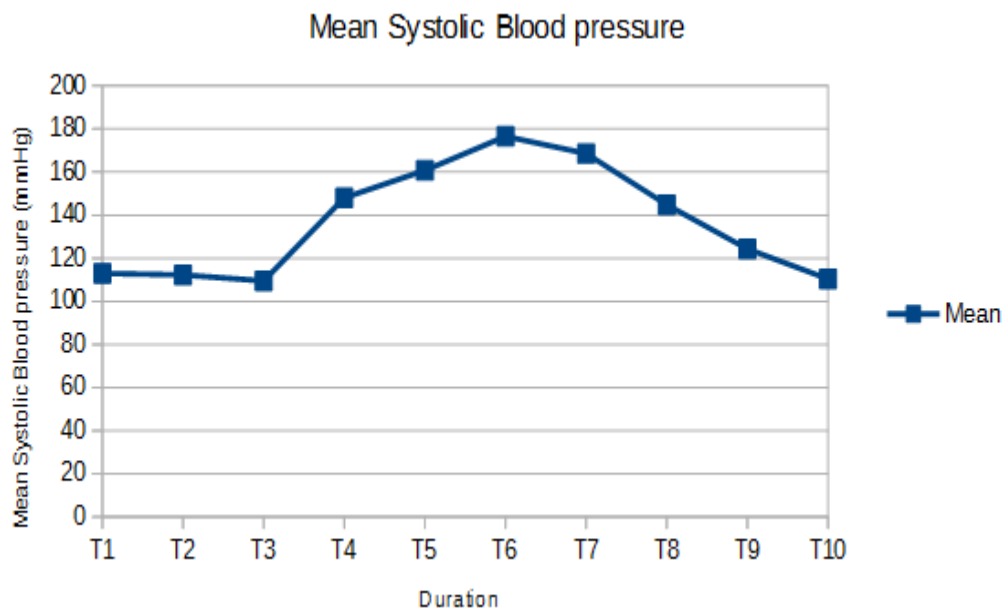


(1c)

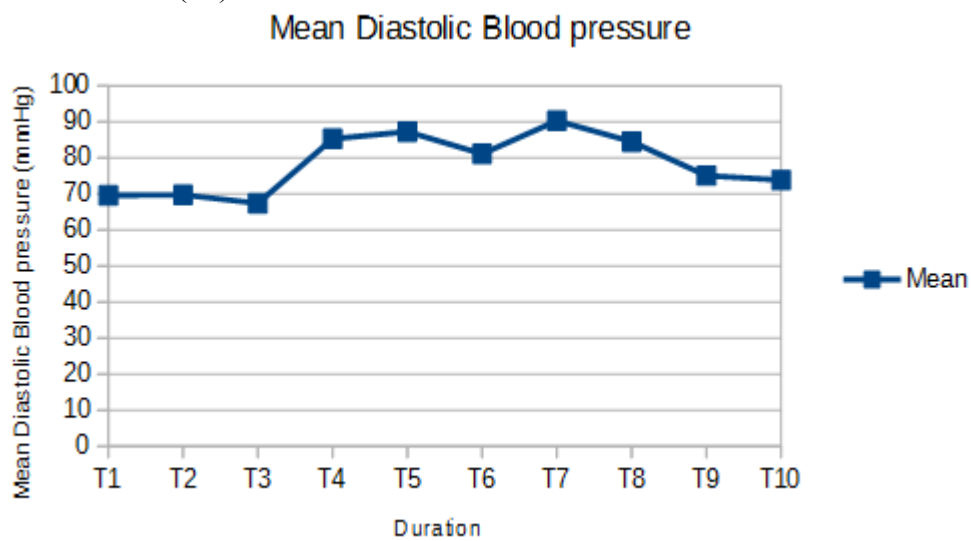
Fig 1. shows the box plot of PTT (a) corresponding sBP(b) and dBP (c) values at measuring points T1 to T10. The boxes represent full range of values.



(2a)

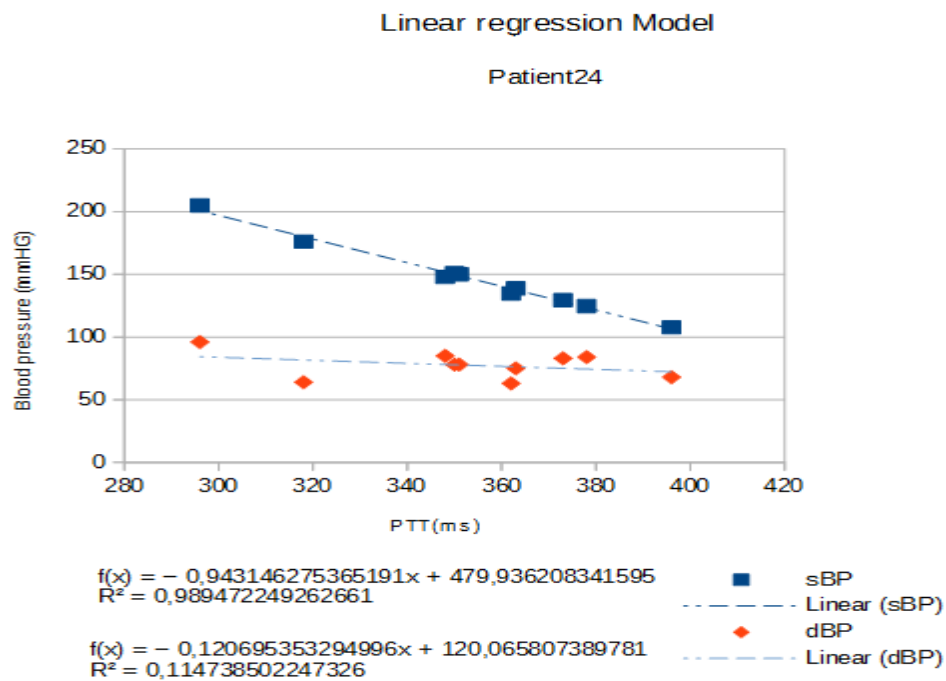


(2b)

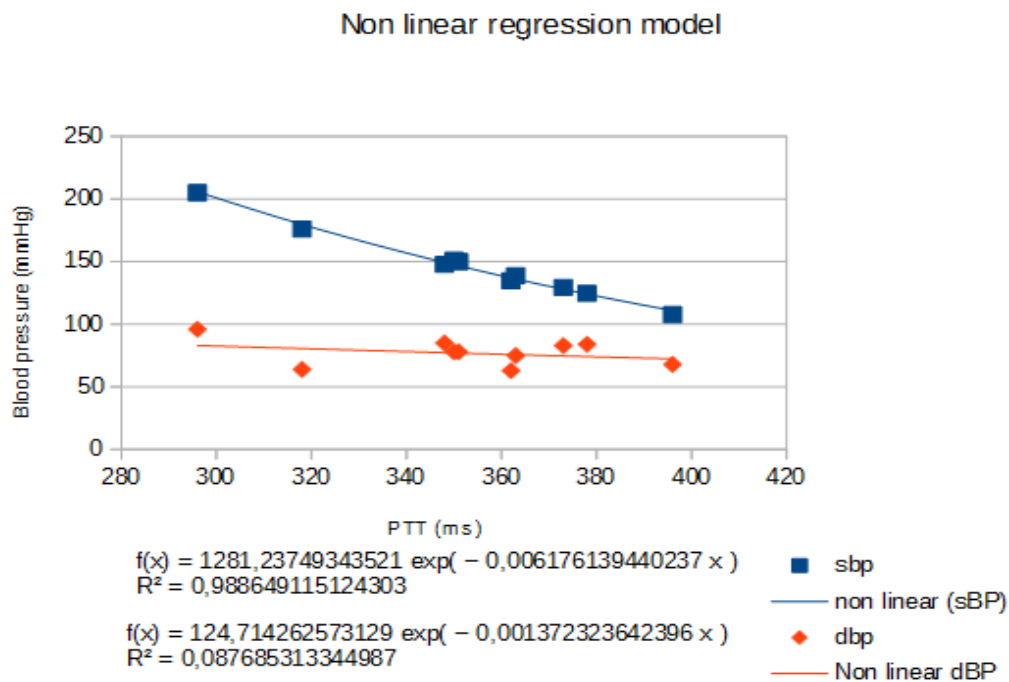


(2c)

Fig 2. shows the mean PTT for patient 6 (a) corresponding sBP (b) and dBP (c)



(3a)



(3b)

Fig 3. shows the relationship between PTT and blood pressure using Linear (a) and non Linear regression model (b) for patient 24.

Mean systolic BP, diastolic BP and PTT at rest were 118 +/- 12 mmHg, 79 +/- 14 mmHg and 354 +/- 36 ms respectively, 190 +/- 35 mmHg, 89 +/- 14 mmHg and 276 +/- 25ms under maximum exercise, and 128 +/- 10 mmHg, 83 +/- 13 mmHg and 371 +/- 38 ms during recovery.

Linear and non-linear regression :

The correlation coefficient between PTT and sBP was calculated with a linear regression model in Table 3a.

[Table 3a]

Patient	Data pairs (n)	r ² Linear regression sBP	r ² Linear regression dBP
1	10	0,948660714285714	0,279017857142857
2	10	0,950782997762864	0,28735632183908
3	10	0,983796296296296	0,275938189845475
4	10	0,936123348017621	0,275330396475771
5	10	0,925925925925926	0,285388127853881
6	10	0,921908893709328	0,276548672566372
7	10	0,983796296296296	0,511363636363636
8	10	0,961538461538462	0,277777777777778
9	10	0,971991341991342	0,51487414187643
10	10	0,983796296296296	0,279017857142857
11	10	0,946547884187082	0,279642058165548
12	10	0,946547884187082	0,53030303030303
13	10	0,965909090909091	0,272331154684096
14	10	0,97926267281106	0,056947608200456
15	10	0,952017543859649	0,273522975929978
16	10	0,957947598253275	0,27114967462039
17	10	0,981991341991342	0,290697674418605
18	10	0,97254004576659	0,277161862527716
19	10	0,923913043478261	0,289351851851852
20	10	0,923913043478261	0,282167042889391
21	10	0,959367945823928	0,288018433179723
22	10	0,955056179775281	0,27292576419214
23	10	0,923913043478261	0,074183976261128
24	10	0,988372093023256	0,114599552572707
25	10	0,988372093023256	0,282805429864253
26	10	0,974770642201835	0,519630484988453
27	10	0,955056179775281	0,063775510204082
28	10	0,946547884187082	0,290697674418605
29	10	0,946547884187082	0,270562770562771
30	10	0,932017543859649	0,27114967462039

The coefficient of determination (R^2) between PTT and sBP was calculated with a non linear regression model in Table 3b.

[Table 3b]

Patient	Data pairs (n)	R^2 Non Linear regression	R^2 Non Linear regression
		sBP	dBP
1	10	0,965909090909091	0,274725274725275
2	10	0,959367945823928	0,278396436525612
3	10	0,946547884187082	0,279017857142857
4	10	0,988372093023256	0,269396551724138
5	10	0,932017543859649	0,27114967462039
6	10	0,927254004576659	0,284738041002278
7	10	0,983796296296296	0,489130434782609
8	10	0,946547884187082	0,269396551724138
9	10	0,915948275862069	0,507900677200903
10	10	0,938189845474614	0,286697247706422
11	10	0,97926267281106	0,278396436525612
12	10	0,981524249422633	0,569767441860465
13	10	0,970319634703196	0,274725274725275
14	10	0,921908893709328	0,05592841163311
15	10	0,986078886310905	0,279017857142857
16	10	0,921908893709328	0,278396436525612
17	10	0,925948275862069	0,275330396475771
18	10	0,925948275862069	0,278396436525612
19	10	0,963718820861678	0,286697247706422
20	10	0,942350332594235	0,277777777777778
21	10	0,938189845474614	0,290697674418605
22	10	0,97926267281106	0,284090909090909
23	10	0,91991341991342	0,059241706161138
24	10	0,988372093023256	0,272331154684096
25	10	0,959367945823928	0,282805429864253
26	10	0,955056179775281	0,523255813953488
27	10	0,950782997762864	0,068119891008174
28	10	0,942350332594235	0,275938189845475
29	10	0,936123348017621	0,269396551724138
30	10	0,929978118161925	0,274725274725275

Linear regression revealed a significant, strong negative correlation (r) between PTT and sBP in all of the 30 patients (r^2 shown in Table 3a). The correlation between PTT and dBP was rather weak.

Non linear best fit curves were calculated and the coefficients of determination (R^2) were estimated. Results for R^2 and r^2 and the calculated best-fit curve for patient 24 is shown in Fig. 3a and 3b. Similar curves were achieved for other patients with ranging from $0.91 < R^2 < 0.99$ and $0.92 < r^2 < 0.99$

Bland-Altman plot

*“In order to more readily see there difference between the two measurement instruments, it is useful to plot the means of each pair of measurements (x value) versus the difference between the measurements (y value). This is called a **Bland-Altman Plot**, and is shown in Figure 4. “*

[5]. Bland-Altman plots for the linear regression model revealed limits of agreement of -10.6 to 10.6 mmHg for sBP and -10.5 to 10.5 mmHg dBP.

Bland-Altman plots for the non linear regression model yielded limits of agreement between -8.5 to 8.5 mmHg fort sBP and -6.6to 6.6 mmHg for dBP.

Blood pressure values above 160 had a higher scatter.

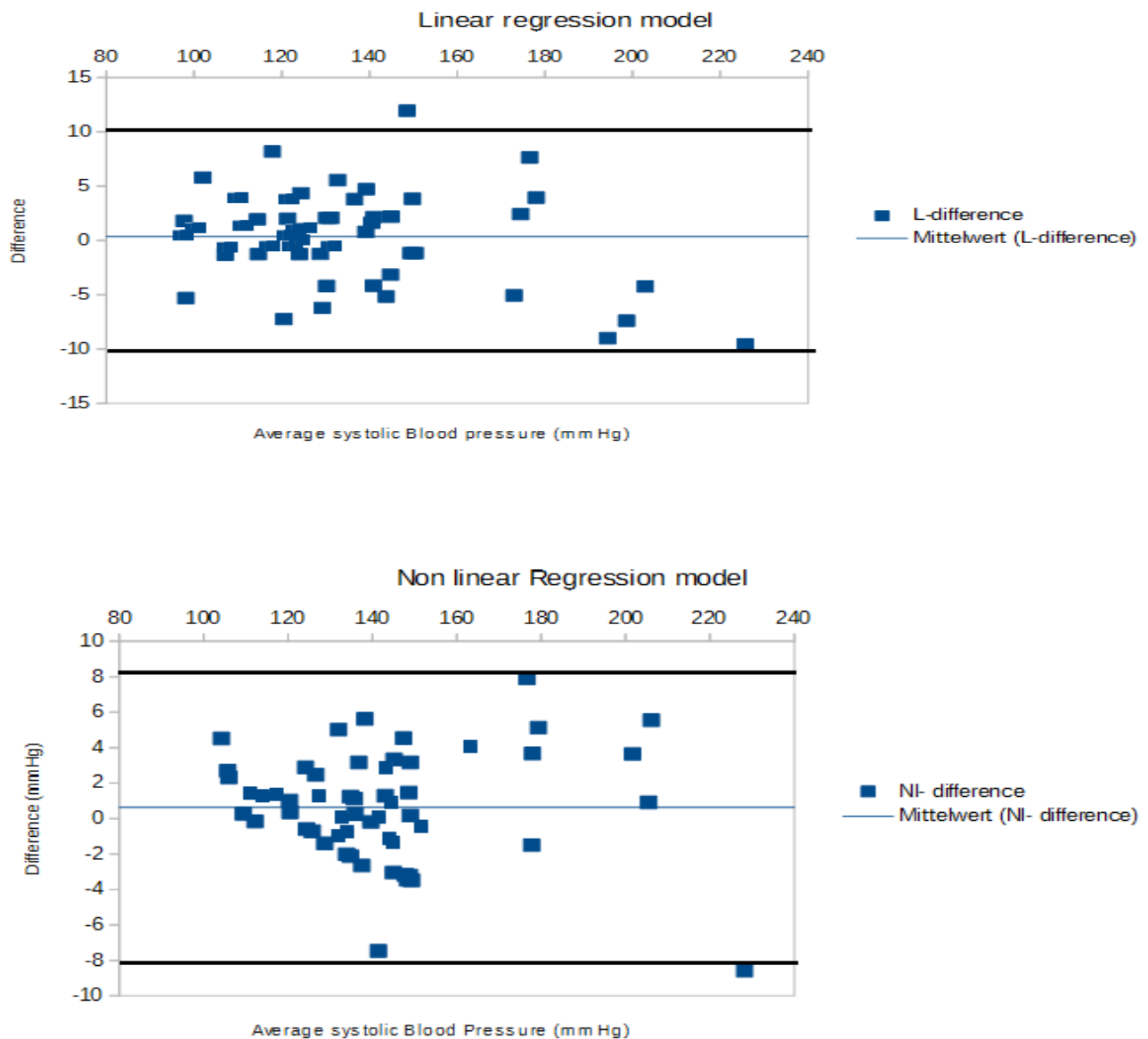


Fig 4. shows the limits of agreement for blood pressure values obtained using Linear (a) and non Linear regression model (b) on a Bland-Altman plot.

1. Jones, Daniel W., et al. "Measuring blood pressure accurately: new and persistent challenges." *Jama* 289.8 (2003): 1027-1030.
2. Mattu, Gurdial S., Balraj S. Heran, and James M. Wright. "Overall accuracy of the BpTRU™—an automated electronic blood pressure device." *Blood pressure monitoring* 9.1 (2004): 47-52.
3. McManus, Richard J., et al. "Telemonitoring and self-management in the control of hypertension (TASMINH2): a randomised controlled trial." *The Lancet* 376.9736 (2010): 163-172.
4. Godwin, Marshall, et al. "Manual and automated office measurements in relation to awake ambulatory blood pressure monitoring." *Family practice* 28.1 (2011): 110-117.
5. <http://www.real-statistics.com/reliability/bland-altman-analysis/bland-altman-plot/>
<https://www.thepensters.com/free-plagiarism-checker-for-students-online.html>